CAMBRIDGE
UNIVERSITY PRESS

Research Paper

Investigation of the coronal heating through phase relation of solar activity indexes

K. J. Li[1,3,4], J. C. Xu[1,3,4], Z. Q. Yin[3,4], J. L. Xie[1,3,4] and W. Feng[2]

[1]Yunnan Observatories, CAS, Kunming 650011, China, [2]Research Center of Analysis and Measurement, Kunming University of Science and Technology, Kunming 650093, China, [3]Center for Astronomical Mega-Science, Chinese Academy of Sciences, Beijing 100012, China and [4]Key Laboratory of Solar Activity, National Astronomical Observatories, CAS, Beijing 100012, China

Abstract

The coronal heating problem is a long-standing perplexing issue. In this study, 13 solar activity indexes are used to investigate their phase relation with the sunspot number (SSN). Only three of them are found to statistically significantly lag the SSN (large-scale magnetic activity) by about one solar rotation period; the three indexes are total solar irradiance (TSI), the modified coronal index, and the solar wind velocity; the former two indexes may represent the long-term variation of energy quantity of the heated photosphere and corona, respectively. The Mount Wilson Sunspot Index (MWSI) and the Magnetic Plage Strength Index (MPSI), which reflect the large- and small-scale magnetic field activities, respectively, are also utilised to investigate their phase relations with the three indexes. The three indexes are found to be much more intimately related to MPSI than to MWSI, and MWSI statistically significantly leads TSI by about one rotation period. The heated corona is found to pulse perfectly in step with the small-scale magnetic activity rather than the large-scale magnetic activity; furthermore, combined with observations, our statistical evidence should thus attribute coronal heating firmly to small-scale magnetic activity phenomena, such as spicules, micro-flares, nano-flares, and others. The photosphere and the corona are synchronously heated, which should seemingly prefer magnetic reconnection heating to wave heating. In the long term, such a coronal heating way is inferred effective. Statistically, it is also small-scale magnetic activity phenomena that produce TSI enhancement. Coronal heating and solar wind acceleration are found to be synchronous, as standard models require.

Keywords: Sun: activity – Sun: atmosphere – Sun: corona

(Received 5 December 2018; revised 30 October 2019; accepted 6 November 2019)

1. Introduction

Total solar irradiance (TSI) varies at all time scales it is measured at present, from minutes to decades, and probably even longer. A variation of about 0.1% in amplitude over a Schwabe cycle is found with satellite observations, and it is believed to mainly come from the combination of two causes: the intensification of bright faculae, plages, and network elements, and the reduction due to the 'blocking' of sunspots (radiating at lower effective temperature) that appear on the visible solar disk. The former cause is slightly dominant around the maximum time of a solar cycle; therefore, TSI is in phase with the Schwabe cycles (Frohlich 2006; Solanki et al. 2013). Hempelmann & Weber (2012) found that the correlation between TSI and the sunspot number (SSN) is strongly nonlinear, and they interpreted this as the net balance between brightening by faculae and darkening by sunspots, with faculae dominating at low activity and sunspots dominating at high activity. Li et al. (2012) found that TSI is statistically more correlated with the network magnetic elements than magnetic fluxes in active regions, implying that the TSI variation should be caused mainly by the small-scale magnetic field. The long-term variation of TSI is still an open issue which need to be further addressed.

Coronal heating is a big question not only in solar physics but also in astrophysics (Arregui 2015; Wilmot-Smith 2015). The issue of solar wind acceleration is generally accompanied by the puzzle of coronal heating (Cranmer, 2012). For decades since the 1940s, extensive studies have been carried out through theory and observations to cope with the coronal heating and solar wind acceleration problems. Modern high-resolution observations tend to attribute coronal heating to small-scale magnetic activities, such as spicules, micro-flares, and nano-flares (Parker 1988; Shibata et al. 2007; Yang et al. 2018). How is the global corona being heated by the small-scale magnetic activities and what is the final effect? Observations have given evidences just through local heating channels, and no other images have been provided to illustrate the global representation of the heated corona. Meanwhile, some theoretical models have been proposed to address this issue at length, and they can be classified into two categories: one is magnetic reconnection energy release and the other is magnetohydrodynamic (MHD) wave heating (Alfven 1947; Parker 1972; Yang et al. 2018). However, it is unknown yet which one is the main mechanism. Further studies are needed on both observations and theoretical models.

Recently, Li et al. (2018) found that among the 985 solar spectral irradiances (SSIs), those form in the upper photosphere, chromosphere, transition region, and corona are more significantly related to small-scale magnetic activity than to large-scale magnetic activity, implying that it should be small-scale magnetic

activity that effectively heats these atmosphere layers. Meanwhile, they found some SSIs are positively correlated, and some others are negatively correlated with small-scale magnetic activity. TSI is defined as the sum of all SSIs. Is TSI more correlated with small- or large-scale magnetic activity?

Coronal heating is closely related to the global magnetic activity on the whole solar surface (De Moortel & Browning 2015); however, magnetic activity temporally changes in short and long terms, and thus the physical situation of the heated corona changes temporally. Therefore, exploring the relationship among indexes of long-term activity on the whole solar disk may somewhat address the issue of coronal heating. In this study, we will not address the issue directly but will do it indirectly by investigating phase relations with almost all solar activity indexes of long-term observations; finally, a special relation will be found, and it provides some clues which answer the above problems from a statistical view.

2. Phase relationship of long-term solar activities

2.1. Data

Daily records of the following 14 solar activity indexes are used to investigate phase relation among them: SSN[a] and sunspot area[b] from 1874 May 9 to 2013 Dec 31, the adjusted 10.7-cm radio flux from 1947 March 5 to 2013 Dec 31 measured by Ottawa/Penticton[1], flare index from 1966 Jan 1 to 2008 Dec 31[1] (Atac 1987), daily mean values of both the equivalent width of the helium 1 083-nm solar absorption line and the absolute line-of-sight magnetic field strength averaged over solar disk which are both measured by NSO/Kitt Peak from 1977 Jan 1 to 2003 Sept 21[1], Ca II 393.3-nm core-to-wing ratio (Ca II index) observed by the Solar-Stellar Irradiance Comparison Experiment from 1991 Oct 3 to 1994 Sept 30[1], X-ray intensity at 1–8 Å measured by the Geostationary Operational Environmental Satellite (GOES) from 1992 Jan 1 to 2001 Dec 31[1], modified coronal index (MCI) constructed on the basis of ground-based measurements of the intensities of the coronal line 530.3 nm from 1943 Jan 1 to 2012 Dec 31[c] (Lukac & Rybansky 2010; Minarovjech et al. 2011), daily mean values of both the interplanetary magnetic field and solar wind velocity measured by various spacecrafts near the Earth's orbit from 1963 Nov 27 to 2013 Dec 31 given by OMNIWeb[1], daily occurrence number of coronal mass ejections (CMEs) from 1996 Jan 11 to 2013 June 30 listed in the SOHO/LASCO CME CATALOG[d], Mg II core-to-wing ratio (Mg II index) from 1978 Nov 17 to 2007 Oct 24[1] (Heath & Schlesinger 1986; Viereck & Puga 1999), and the PMOD composite of TSI from 1978 Nov 17 to 2007 Oct 24[1] (Frohlich 2006). They are shown in Figure 1. SSN is utilised to represent long-term variation of solar activity, and its time interval covers any time span of the rest indexes.

2.2. Phase relationship of 14 solar activity indexes

In order to study the phase relationship between daily SSN and the other 13 indexes, we performed lagged cross-correlation analyses

between the former and each of the latter ones, respectively. The algorithm of lagged cross-correlation is briefly described as follows. First, we adjust the lengths of the two considered time series, so that they cover a common time interval. Specifically, the time series of SSN is truncated to match the time interval of the other series. We calculate the cross-correlation coefficient (cc) between the two time series. This is cc at the shift of zero day, when there is no relative movement between the two time series. Second, one series is 1 d shifted with respect to the other. The unpaired data points are deleted. We then obtain a new value of cc. This is the case at the shift of 1 d. Third, one series is 2 d shifted with respect to the other. Similarly, the unpaired data points are deleted, and we obtain another new cc value. This is the case at the shift of 2 d, and so on. If no observation on a certain day is measured for either of the two time series, then the record for that day is set to be a negative value in the time series, and any negative value should not take part in the calculation of cc. Figures 2, 3, and 4 show the obtained results, where the abscissa shows shifts of SSN against the other indexes with backward shifts given negative values. In the top panel of Figure 4, the cc value of SSN with TSI plus 0.28 is shown to give a clear display. Except these three indexes, TSI, MCI, and solar wind velocity, the rest 10 solar activity indexes have the largest cc (the absolute value) with SSN when the relative phase shift is about zero. However, for TSI and MCI, the maximal cc (cc_{peak}) does not coincide with the local maximum of ccs around shifts of zero (cc_0); for these two, cc is the largest when SSN leads them by 29 and 27 d, respectively. This means that SSN should lead TSI and MCI by about one solar rotation period. For solar wind velocity which is measured around the Earth orbit, the absolute value of cc reaches local maximum when SSN leads by 5 d, implying that the travel time of solar wind should statistically be about 5 d from the Sun to the Earth. The absolute value of cc reaches the largest when SSN leads solar wind velocity by 32 d, implying that SSN should lead solar wind velocity by about one rotation period.

In order to test the statistical significance of the difference between two correlation coefficients, cc_0 and cc_{peak}, the Fisher translation method (Fisher 1915) is carried out in the same way as Li et al. (2002, 2014, 2018) did. Resultantly for the two time series, TSI and SSN, the difference between the two coefficients is found to be significant with a probability of about 100%. For MCI and SSN, the difference between the two coefficients is significant with a probability of about 99%, and for the solar wind velocity and SSN, it is significant with a probability of about 99%.

In general, the above phase relationship of long-term solar activity displays that long-term variations of TSI, MCI, and solar wind velocity are not mainly or directly caused by large-scale magnetic field activity. Usually, the large-scale strong magnetic field in sunspots should decay to small-scale weak magnetic field after a solar rotation; thus, such phase leads of the three indexes indicate that they should be more correlated with small-scale magnetic activity than to large-scale magnetic activity.

2.3. Statistical view for small-scale magnetic activity heating the solar corona

At Mount Wilson Observatory, two magnetic indexes, the Mount Wilson Sunspot Index (MWSI) and the Magnetic Plage Strength Index (MPSI), are calculated with daily magnetograms observed at its 150-foot solar tower (Howard 1980). To calculate the MPSI from the magnetogram of a certain day, the absolute magnetic field strengths of all of the pixels that is between 10 and 100
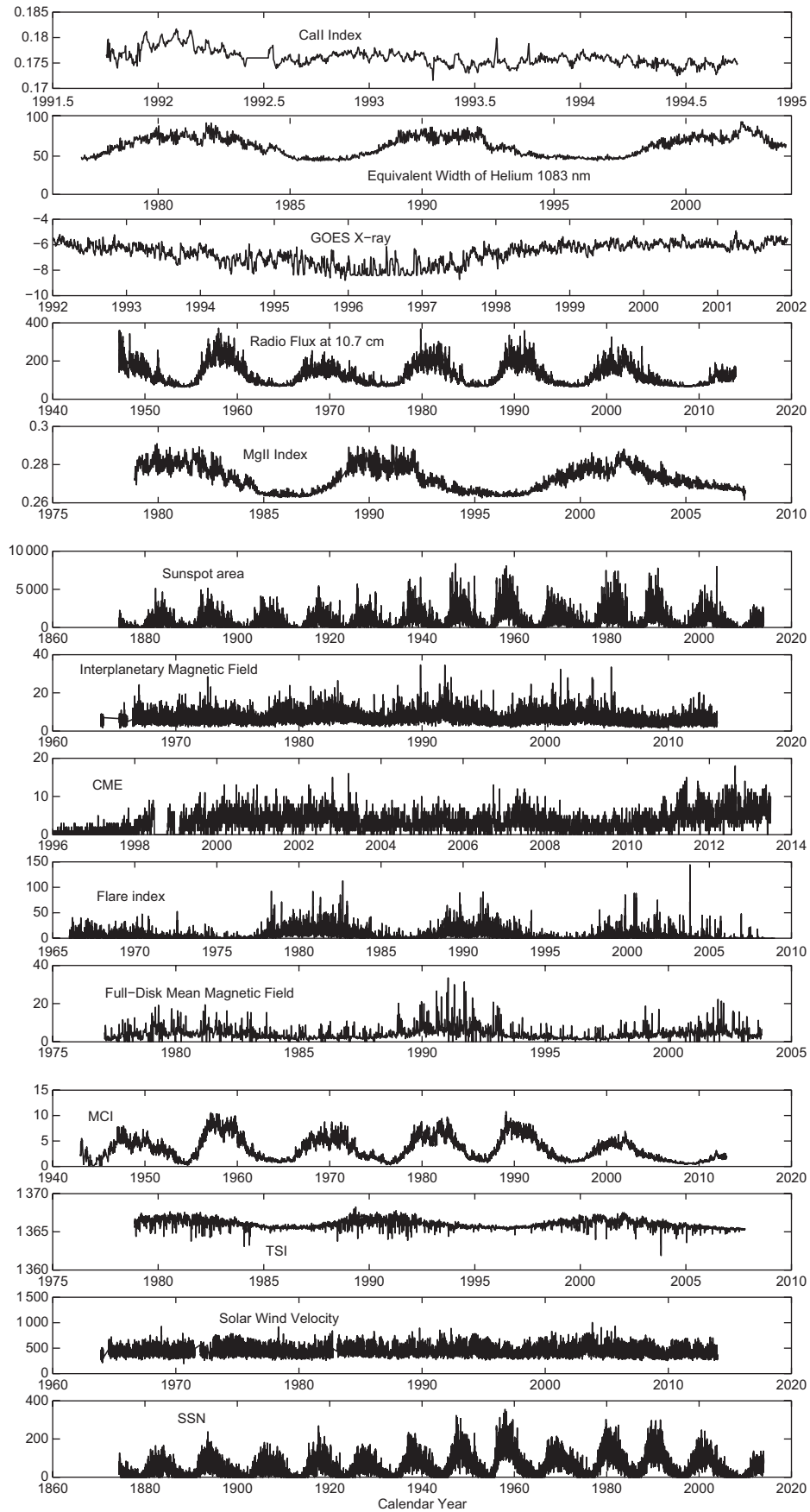
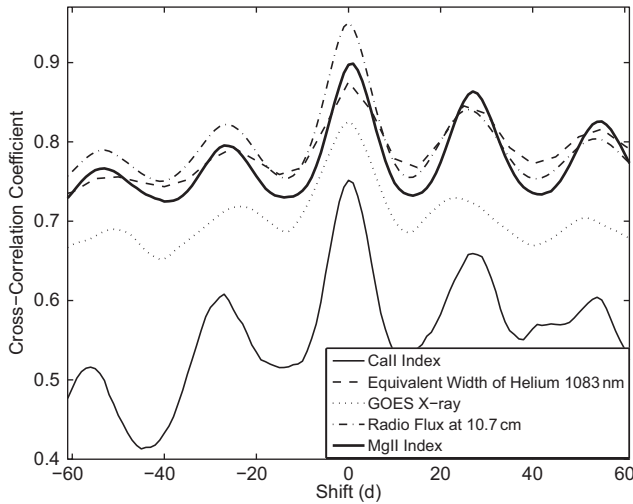**Figure 1.** Fourteen long-term solar activity indexes.

Figure 2. Cross-correlation coefficient between the daily sunspot number (SSN) and the Ca II index (thin solid line), the equivalent width of the helium 1 083 nm (dashed line), the GOES X-ray intensity at 1–8 Å (dotted line), the adjusted 10.7-cm radio flux (dashed and dotted line), and the Mg II index (thick solid line), respectively, varying with their relative phase shifts with backward shifts giving negative values.
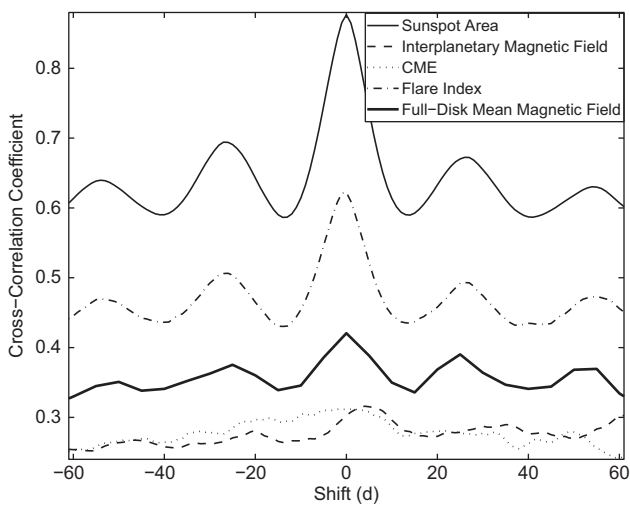

Figure 3. Cross-correlation coefficient between the daily sunspot number (SSN) with the sunspot area (thin solid line), the interplanetary magnetic field (dashed line), the daily occurrence number of coronal mass ejections (CMEs, dotted line), the flare index (dashed and dotted line), and the full-disk mean line-of-sight magnetic field strength (thick solid line), respectively, varying with their relative phase shifts with backward shifts giving negative values.

Gauss are summed up and divided by the total number of pixels. MWSI is calculated similarly, but for pixels whose absolute values are greater than 100 Gauss[5]. MWSI should thus represent large-scale magnetic field activity mainly in sunspot regions at the solar full disk, while MPSI represents small-scale magnetic field activity outside sunspot regions (Xiang et al. 2014; Xiang & Qu 2016). Figure 5 shows MPSI and MWSI from 1970 Jan 19 to 2012 Dec 31. During the total 15 688 d, the two indexes are measured in 11 320 d, accounting for 72.2%; they are used to perform lagged cross-correlation analyses, respectively, with TSI,
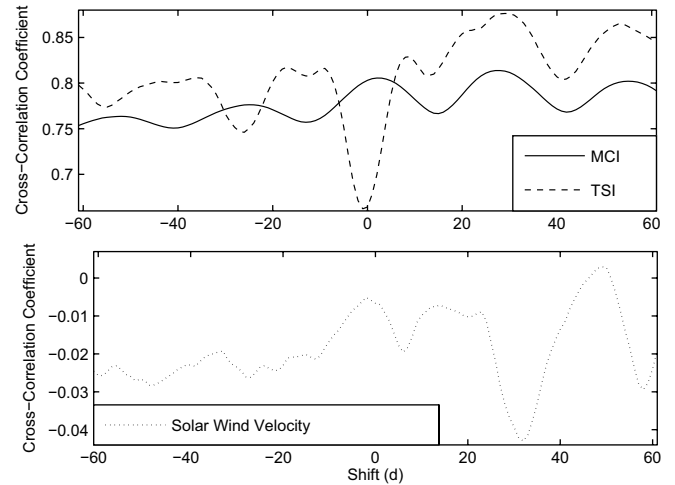
Figure 4. Cross-correlation coefficient between the daily sunspot number (SSN) and the modified coronal index (MCI, solid line), the total solar irradiance (TSI, dashed line), and the solar wind velocity (dotted line), respectively, varying with their relative phase shifts with backward shifts giving negative values.
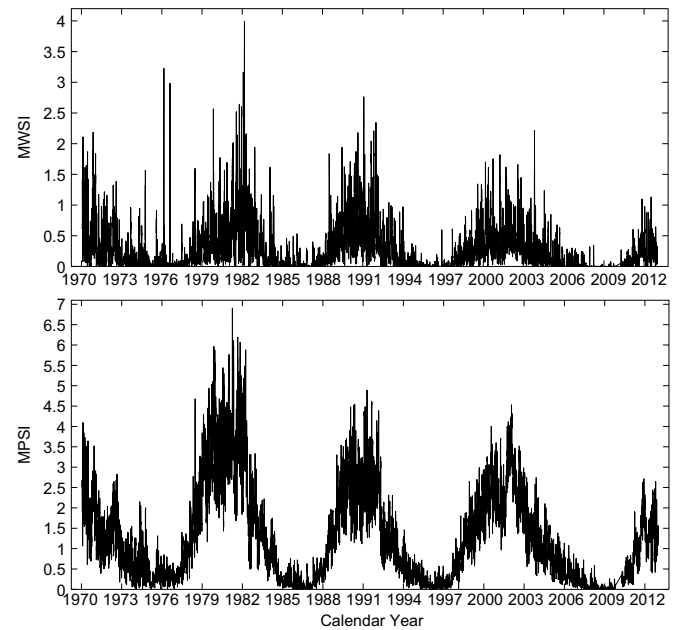

Figure 5. Top panel: daily Mount Wilson Sunspot Index (MWSI). Bottom panel: daily Magnetic Plage Strength Index (MPSI).

MCI, and the solar wind velocity. Figures 6, 7, and 8 show the obtained cross-correlograms, where the abscissa shows shifts of MPSI (or MWSI) versus the three indexes with backward shifts given negative values.

The common time interval of TSI and MPSI spans from 1978 Dec 17 to 2007 Oct 24, i.e., 10 569 d in all. However, on 2 745 d, there are no records for MPSI (or MWSI), which amounts to 26.0%; and on 674 d, there are no records for TSI, which amounts to 6.4%. At no shift, *cc* between MPSI and TSI is 0.5816 (significant at the 99.9% confidence level), which is much larger than that between MWSI and TSI, 0.0254 (statistically insignificant). Therefore, TSI is much more closely related to small-scale magnetic field activity than to large-scale magnetic field activity. At the shift of about 32 d, *cc* between MWSI and TSI reaches its
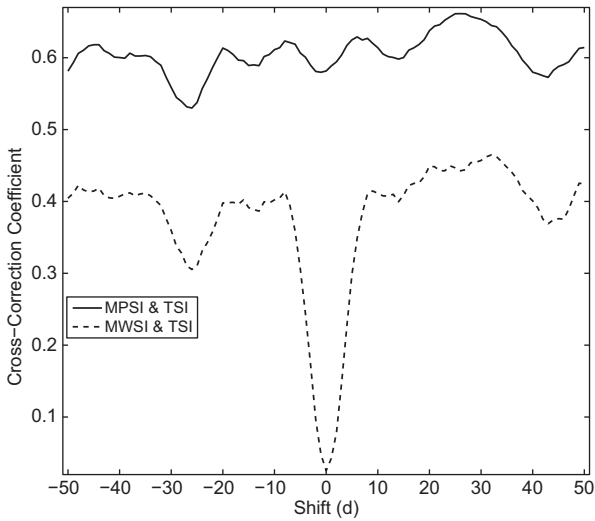
Figure 6. Cross-correlation coefficient between TSI and MPSI (solid), MWSI (dashed), respectively, varying with their relative phase shifts with forward shifts giving negative values.
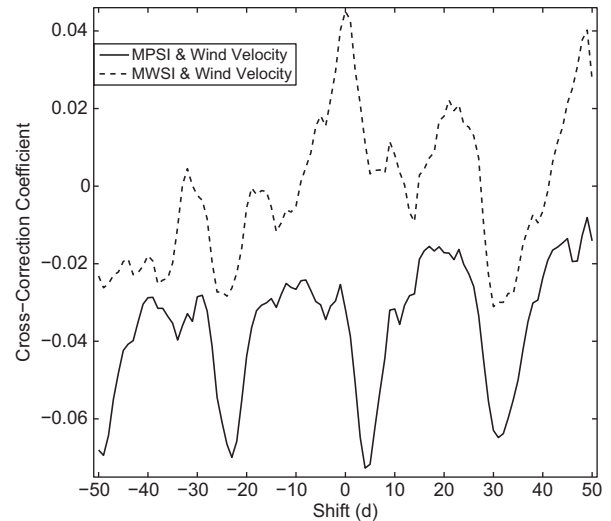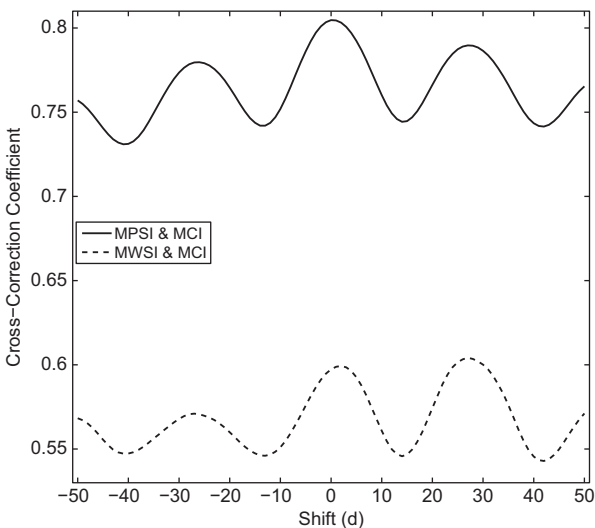

Figure 7. Same as Figure 6, but between MCI and MPSI (solid), MWSI (dashed), respectively.

maximum, 0.4648 (statistically significant), which is much larger than that at no shift, indicating that the large-scale magnetic field activity should lead TSI by about one rotation period.

At no shift, cc between MPSI and MCI is 0.8047, which is obviously much larger than that between MWSI and MCI, 0.5963. Therefore, MCI is much more closely related to small-scale magnetic field activity than to large-scale magnetic field activity. At the shift of about 27 d, cc between MWSI and MCI reaches the peak at 0.6032, which is slightly larger than that at no shift.

In the common time interval of the wind velocity and MPSI spanning from 1970 Jan 19 to 2012 Dec 31 with 15 688 d altogether, on 2 086 d there are no records for the solar wind velocity, which amounts to 13.3%. The cc between MPSI and wind velocity is -0.0317 at no shift, and it reaches a local minimum of -0.0727 when MPSI leads by about 4 d, which is of significance at the 95% confidence level. The cc between MWSI and the wind velocity is

Figure 8. Same as Figure 6, but between the solar wind velocity and MPSI (solid), MWSI (dashed), respectively.

0.045 at no shift, and it reaches a local minimum of 4.19×10^{-3} at the shift of about 7 d. When MWSI leads by about 30 d, cc has the minimum value, -0.031. For MWSI, these three values are statistically insignificant. Therefore, the wind velocity is much more clearly related to small-scale magnetic field activity than to large-scale magnetic field activity.

3. Special phase relationship of solar activities at the extended minimum of the current cycle

The minimum of the current cycle (cycle 24) is much deeper than previous ones in the modern era, and no or just a few sunspots appear at the disk for about 3 yr (2007–2009) during this extended solar minimum (Li et al. 2011). Next, we want to know whether the aforementioned phase lead takes place or not during the time interval.

Figure 9 displays daily SSN from 2007 Jan 1 to 2009 Dec 31. As the figure shows, SSN is less than 20 at the time interval of 2008 Apr 5 to 2009 Dec 8, and here it is utilised to investigate phase relationship with TSI, MCI, and solar wind velocity in the interval.

Figure 10 shows the obtained results. The largest cross-correlation coefficient (cc) between MCI and SSN appears around a relative phase shift of zero. TSI has the largest cc with SSN, 0.283, when the relative phase shift is 5 d. At the relative phase shift of zero, the cc between TSI and SSN is 0.211.

For the solar wind velocity, the absolute value of cc reaches the local maximum when SSN leads by 1 d, and meanwhile $cc = -0.114$, but $cc_0 = -0.099$ when relative phase shift is zero. The absolute value of cc reaches the largest when SSN lags by 17 d, and meanwhile $cc_{peak} = -0.121$. The theoretical calculation for statistical significance examination shows that $\delta z = 0.275\sigma$, and the difference between the two coefficients is significant with a probability of about 78%. The difference between cc_0 and cc_{peak} is statistically insignificant.

Therefore, during the minimum time of cycle 24 when the solar activity is very low, the phase relation that SSN leading the three indexes (TSI, MCI, and solar wind velocity) by about a solar rotation does not exist.
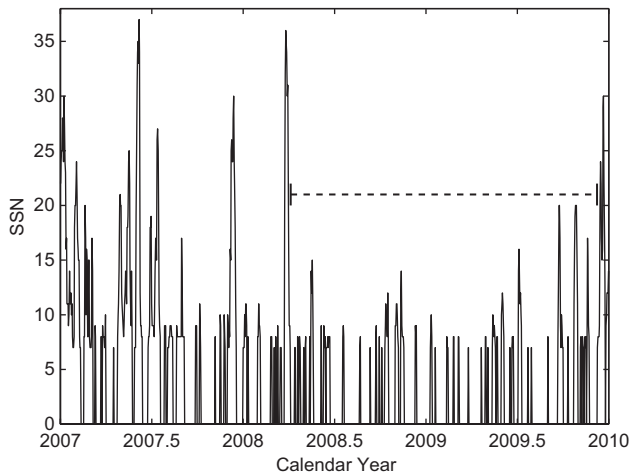
Figure 9. Daily sunspot number (SSN, solid line) from 2007 Jan 1 to 2009 Dec 31. SSN is less than 20 at the time interval from 2008 Apr 5 to 2009 Dec 8, which is marked by the dashed thick horizontal line.
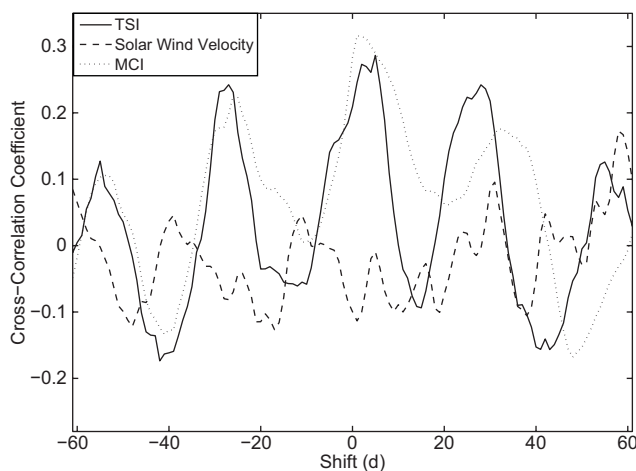

Figure 10. Cross-correlation coefficient (*cc*) between daily sunspot number (SSN) at the time interval of 2008 Apr 5 to 2009 Dec 8 and the total solar irradiance (TSI, solid line), the modified coronal index (MCI, dotted line), and the solar wind velocity (dashed line), respectively, varying with their relative phase shifts with backward shifts giving negative values.

4. Conclusions and discussion

The Sun's atmosphere is magnetic; its large-scale magnetic activity is shown by sunspot regions, and its small-scale magnetic activity is manifested mainly by ephemeral regions and network and intra-network magnetic elements. The SSN has a continuous and the longest record, and it is thus used here to represent the long-term activity of large-scale solar magnetic activity. Daily SSN from 1874 May 9 to 2013 Dec 31 is utilised to investigate phase relationship, respectively, with 13 daily solar activity indexes, and it is found that except the three of them, TSI, MCI, and solar wind velocity, the other 10 indexes are in phase with SSN. However, for these three indexes, SSN should statistically significantly lead themselves in phase angle by about one solar rotation period. This indicates that the long-term variation of the three indexes should statistically synchronously arise from the same activity, and they are not directly connected with the large-scale magnetic field activity.

Furthermore, two daily magnetic indexes which come from direct observations (magnetograms) of solar magnetic fields at the solar full disk, the MWSI and the MPSI, are utilised to investigate the phase relation, respectively, with the three indexes. MWSI may represent large-scale magnetic field activity, while MPSI represents small-scale magnetic field activity. MPSI is found much more closely related to the three indexes than MWSI does. MWSI should seemingly lead the three indexes by about one rotation period, but such a lead is of statistical significance just for TSI.

MCI is an energy-related index that represents the average irradiance (power) emitted by the green corona (Minarovjech et al. 2011), and its time series may resemble the long-term variation of the corona energy, namely the variation of temperature at a certain layer of the corona. The phase relation between TSI, MCI, and large-scale solar magnetic activity reveals that there should be a certain mechanism which heats the photosphere and corona synchronously, so that their long-term variation maintains such a relation consistently. The strong relation of both TSI and MCI with small-scale magnetic activity implies that coronal and photospheric heating should be possibly related with small-scale magnetic activity. High-resolution observations and theoretical studies during the recent several decades ascribe coronal heating firmly to small-scale weak magnetic activity phenomena (events), such as spicules, micro-flares, and nano-flares (Golub et al. 1974; Parker 1988; Shibata et al. 2007; Zhang & Liu 2011; De Moortel & Browning 2015; Tavabi et al. 2015; Tavabi 2018). The time series of MPSI reflects the temporal occurrence frequency of small-scale weak magnetic activity events which are related to small-scale magnetic fields, while SSN could reflect the occurrence frequency of large-scale magnetic activity events (flares, CMEs, and so on). The large-scale magnetic structures should be first observed when they appear on the solar surface. Their evolutional component should be observed as the disintegrated small-scale magnetic structures (elements) that appear again on the visible solar disk after a rotation. Thus, it is mainly the disintegrated components of sunspot regions that bring about the cyclical variation of coronal heating, and our findings statistically give such an evidence. In other words, observations manifest small-scale weak magnetic activity events as channels of heating the corona, and our statistical analysis further manifests the practical efficiency of such heating channels: the heated corona shares the same breath with weak magnetic activity phenomena. This result is in agreement with that given by Li et al. (2018).

Spruit & Zwaan (1981) found that the smaller the magnetic features are, the brighter they are. Thus, the small-scale magnetic activity should contribute mainly in increasing TSI. Li et al. (2012) also found that TSI is more related with the small-scale magnetic field activity (network magnetic elements) than the large-scale magnetic field activity (magnetic fluxes in active regions). Hot plasmas are observed to flow along ultra-fine loops from the photosphere upward to the base of the solar corona, and their individual foot-points are located in the inter-granular lanes. Therefore, dynamical events are directly observed to originate in small-scale magnetic field elements of the photosphere and subsequently through small-scale magnetic foots to impulsively light up the solar corona (Ji et al. 2012). Tavabi (2018) found a robust correlation among network bright points at all layers from the photosphere to corona, and he inferred that small-scale magnetic field concentrations should be responsible for the relationship. Therefore, observations confirm that the photosphere and corona should be synchronously heated by small-scale magnetic activity

events. The long-term variation of TSI should be caused mainly by the heating of small-scale magnetic activity events.

Although observations have displayed the contribution of MHD waves in heating the corona, the mechanism of MHD wave heating should seemingly be excluded from being the main one—this is because the mechanism could hardly explain the phase relation between MCI, TSI, and large-scale solar magnetic activity (SSN), and the much closer relation between MCI, TSI, and small-scale magnetic activity (MPSI) than large-scale activity (SSN and/or MWSI). After we excluded the MHD wave mechanism, the alternative mechanism, reconnection, is the only plausible explanation for coronal heating.

Slow-velocity wind is positively correlated with SSN, while fast-velocity wind is negatively correlated with the latter (Li et al. 2016). Therefore, the negative correlation of solar wind velocity, respectively, with SSN, MPSI, and MWSI in this study should primarily reflect the behaviour of fast-velocity wind. Large coronal holes (CHs) contain large numbers of rapidly varying bright points that often coincide with the boundaries of super-granular cells, and these network-edge regions in CHs are regarded as possible 'launching' sites for the fast wind (Cranmer, 2009). The source regions of the fast solar wind were identified in the polar CH (Hassler et al. 1999; Wilhelm et al. 2000).

Furthermore, fast wind should emanate from coronal funnels in CHs, which are rooted near super-granulation boundaries in the network lanes, through reconnection with the magnetic fields of nearby small-scale loops (Tu et al. 2005). It is observed that CHs persist as large northern and southern polar caps for approximate 7 yr around the minimum of a solar cycle Cranmer (2009). They expand towards the heliographic equator during the declining phase of each Schwabe cycle and shrink back to the poles in the rising phase of the successive cycle (Waldmeier 1981; Das et al. 1993). Polar CHs disappear during the maximum solar activity phase for a certain time and reappear with an inverted magnetic field polarity (Storini et al. 2006). Thus, large CH activity is in anti-phase with solar cycles (Wang 2012). Fast wind is closely associated with open magnetic field regions of CHs (Wang 2012); thus, fast wind velocity should also be in anti-phase with the solar activity cycles, and that is why wind velocity is negatively correlated with MPSI (SSN and MWSI). Porter et al. (1987) and Martin (1988) suggested that the energy source for heating the corona and accelerating solar wind should most likely be the dynamic network field, which was also amply described by Parker (1972, 1991). Standard models display the same subsequent requirement on coronal heating as on solar wind acceleration (Wilhelm et al. 2000; Tu et al. 2005). Here, we corroborate that this requirement is statistically valid: coronal heating and wind acceleration are synchronous and related to the small-scale magnetic activities. Besides, it is revealed that the fast solar wind emanates from large holes mainly by small-scale magnetic activities through magnetic reconnection. Fast solar wind may also blow out from active regions which are in anti-phase with polar CHs (Wang 2012), and this is the main reason why the correlation coefficients of solar wind of high velocity separately with SSN and MPSI are not very large, although the correlations are of statistical significance. Moreover, solar wind acceleration and coronal heating can be observed simultaneously, and the relation of solar wind with small-scale magnetic activity thus exists.

This study aims at the long-term variations of solar active indexes, and original series used here may include short-term variations. For example, TSI and SSN are positively correlated with

each other on the scale of a sunspot cycle and longer but negatively related on the scale of years and shorter (Li et al. 2012). Without excluding short-term fluctuations, MCI, TSI, and fast wind can still be clearly distinguished to vary synchronously with small-scale magnetic activity, and thus their long-term variations are found to be in phase.

After a rotation, strong magnetic activity should generally reappear on the solar visible disk as small-scale magnetic activity. Up to a quarter of the MPSI/MWSI data are missing, which should seriously impact the reappearance, and this is inferred to be the reason why the above phase lead is of statistical insignificance for MCI and solar wind.

Summarising, this study statistically gives an evidence for variations of coronal heating, solar wind acceleration, and TSI enhancement in solar cycles synchronously arising from the same source, i.e., small-scale magnetic activities (events). Here, they are reflected by MPSI and closely related to small-scale magnetic structures. After a solar rotation, large-scale magnetic structures generally become small-scale magnetic elements, so SSN and MWSI lead MCI, TSI, and wind velocity by about a rotation. During the extended minimum of the current cycle, no large-scale strong magnetic structures appear on the solar disk, so the phase lead is not found in the time interval.

References

Alfven, H. 1947, MNRAS, 107, 211. doi: 10.1093/mnras/107.2.211

Arregui, I. 2015, Philosophical Transactions of the Royal Society A: Mathematical, Physical and Engineering Sciences, 373, 20140261. doi: 10.1098/rsta.2014.0261

Atac, T., 1987 Astrophysics Space Science, 135, 201. doi: 10.1007/BF00644477

Cranmer, S. R. 2009, Living Reviews in Solar Physics, 6, 1. doi: 10.12942/lrsp-2009-3

Cranmer, S. R. 2012, Space Sci. Rev., 172, 145. doi: 10.1007/s11214-010-9674-7

Das, T. K., Chatterjee, T. N., & Sen, A. K. 1993, SoPh, 148, 61. doi: 10.1007/BF00675535

De Moortel, I., & Browning P. 2015, Philosophical Transactions of the Royal Society A: Mathematical, Physical and Engineering Sciences, 373, 20140269. doi: 10.1098/rsta.2014.0269

Fisher, R. A. 1915, Biometrika, 10, 507. doi: 10.1093/biomet/10.4.507

Frohlich, C. 2006, Space Sci. Rev., 125, 53. doi: 10.1007/s11214-006-9046-5

Golub, L., Krieger, A. S., Silk, J. K., Timothy, A. F., & Vaiana, G. S. 1974, ApJ, 189, L93. https://ui.adsabs.harvard.edu/abs/1974ApJ...189L..93G/abstract

Hassler, D. M., Dammasch, I. E., Lemaire, P., et al. 1999, Science 283, 810. doi: 10.1126/science.283.5403.810

Heath, D. F., & Schlesinger, B. M. 1986, JGR, 91, 8672. doi: 10.1029/JD091iD08p08672

Hempelmann, A., & Weber, W. 2012, SoPh, 277, 417. doi: 10.1007/s11207-011-9905-4

Howard, R. 1980, Quarterly Bulletin on Solar Activity, 203, 275. https://ui.adsabs.harvard.edu/abs/1980QBSA..203..275H/abstract

Ji, H. S., Cao, W. D., & Goode, P. R. 2012, ApJ, 750, L25. doi: 10.1088/2041-8205/750/1/L25

Li, K. J., Feng, W., Liang, H. F., Zhan, L. S., & Gao, P. X. 2011, Annales Geophysicae, 29, 341. doi: 10.5194/angeo-29-341-2011

Li, K. J., Feng, W., Xu J. C., et al. 2012, ApJ, 747, 135. doi: 10.1088/0004-637X/747/2/135

Li, K. J., Irie, M., Wang J. X., et al. 2002, Publ. Astron. Soc. Japan, 54, 787. doi: 10.1093/pasj/54.5.787

Li, K. J., Kong, D. F., Liang H. F., Feng W. 2014, Astron. Nachr., 335, 371. doi: doi:10.1002/asna.201312016

Li, K. J., Zhanng, J., & Feng, W. 2016, AJ, 151, 128. doi: 10.3847/0004-6256/151/5/128

Li, K. J., Xu, J. C., & Feng, W. 2018, ApJSS, 237, 7. doi: 10.3847/1538-4365/aac7c8

Lukac, B., & Rybansky, M. 2010, SoPh, 263, 43. doi: 10.1007/s11207-010-9545-0

Martin, S. F. 1988, SoPh, 117, 243. doi: 10.1007/BF00147246

Minarovjech, M., Rusin, V., & Saniga, M. 2011, Contrib. Astron. Obs. Skalnate Pleso, 41, 137. https://ui.adsabs.harvard.edu/abs/2011CoSka..41..137M/abstract

Parker, E. N. 1972, ApJ, 174, 499. doi: 10.1086/151512

Parker, E. N. 1988, ApJ, 330, 474. doi: doi:10.1086/166485

Parker, E. N. 1991, ApJ, 372, 719. doi: doi:10.1086/170015

Porter, J. G., Moore, R. L., Reichmann, E. J., Engvold, O., & Harvey, K. L. 1987, ApJ, 323, 380. doi: 10.1086/165835

Shibata, K., Nakamura, T., Matsumoto, T., et al. 2007, Science, 318, 1591. doi: 10.1126/science.1146708

Solanki, S. K., Krivova, N. A., & Haigh, J. D. 2013, Ann. Rev. of Astron. and Astrophys., 51, 311. doi: 10.1146/annurev-astro-082812-141007

Spruit, H. C., & Zwaan, C. 1981, SoPh, 70, 207. doi: 10.1007/BF00151329

Storini, M., Hofer, M. Y., & Sykora, J. 2006, Advances in Space Research, 38, 912. doi: http://doi.org/10.1016/j.asr.2006.03.024

Tavabi, E., Koutchmy, S., & Golub, L. 2015, SoPh, 290, 2871. doi: 10.1007/s11207-015-0771-3

Tavabi, E. 2018, MNRAS, 476, 868. doi: 10.1093/mnras/sty020

Tu, C. Y., Zhou, C., Marsch, E., et al. 2005, Science 308, 519. doi: 10.1126/science.1109447

Waldmeier, M. 1981, SoPh, 70, 251. doi: 10.1007/BF00151332

Wang, Y. M. 2012, Space Sci. Rev., 172, 123. doi: 10.1007/s11214-010-9733-0

Wilhelm, K., Dammasch, I. E., Marsch, E., & Hassler, D. M. 2000, *A&A*, 353, 749. http://aa.springer.de/papers/0353002/2300749/small.htm

Wilmot-Smith, A. L. 2015, Philosophical Transactions of the Royal Society A: Mathematical, Physical and Engineering Sciences, 373, 20140265. doi: 10.1098/rsta.2014.0265

Viereck, R. A., & Puga, L. C. 1999, JGR, 104, 9995. doi: 10.1029/1998JA900163

Xiang, N. B., Qu, Z. N., & Zhai, Q. 2014, AJ, 148, 12. doi: 10.1088/0004-6256/148/1/12

Xiang, N. B., & Qu, Z. N. 2016, AJ, 151, 3. doi: 10.3847/0004-6256/151/3/76

Yang, K. E, Longcope, D. W., Ding, M. D., & Guo, Y. 2018, NatCo, 9, 692. doi: 10.1038/s41467-018-03056-8

Zhang, J., & Liu, Y. 2011, ApJL, 741, L7. doi: 10.1088/2041-8205/741/1/L7